Specular Reflection of Very Slow Metastable Neon Atoms from a Solid Surface

Fujio Shimizu
Institute for Laser Science and CREST, University of Electro-Communications, Chofu-shi, Tokyo 182-8585, Japan
(Received 7 July 2000)

An ultracold narrow atomic beam of metastable neon in the $1s_3[(2s)^5 3p:{}^1P_0]$ state is used to study specular reflection of atoms from a solid surface at extremely slow incident velocity. The reflectivity on a silicon (1,0,0) surface and a BK7 glass surface is measured at the normal incident velocity between 1 mm/s and 3 cm/s. The reflectivity above 30% is observed at about 1 mm/s. The observed velocity dependence is explained semiquantitatively by the quantum reflection that is caused by the attractive Casimir–van der Waals potential of the atom-surface interaction.

DOI: 10.1103/PhysRevLett.86.987 PACS numbers: 34.50.Dy, 03.75.–b, 34.20.Cf

The interaction potential of a neutral atom on a solid surface at a distance much longer than the atomic distance is usually a power-law attractive potential. For the distance shorter than the wavelength of atomic transitions the interaction is the van der Waals potential [1] of the form $U_{\text{int}} = -C_3/r^3$, where r is the distance of the atom from the surface. At a larger distance it becomes $U_{\text{int}} = -C_4/r^4$ due to the retardation of the electrostatic interaction, which was derived by Casimir *et al.* [2]. The crossover occurs at about the distance $r \sim \lambda/2\pi$, where λ is the effective atomic transition wavelength that contributes to the polarizability. The van der Waals potential has been extensively studied because of its relevance to the adsorption of atoms on solid surfaces [3]. Its magnitude has been determined by various techniques [4–13]. It has also been estimated indirectly from the adsorption coefficient. The trajectory of atoms in those experiments is basically governed by the classical mechanics, where the atom moves in the classical attractive potential U_{int}. On a flat surface the atom will collide ultimately on the repulsive wall of the surface potential and is scattered or adsorbed.

When the atomic motion is sufficiently slow, however, the wave nature becomes important. The atom can be reflected back at a steep slope of the potential if the spatial variation of the local wave vector $k = \sqrt{\{k_0^2 - 2mU_{\text{int}}/\hbar^2\}}$ is sufficiently abrupt regardless of the sign of the variation, where k_0 is the wave vector of the atom normal to the surface at $r \to \infty$. This condition states that the variation of k within the distance of the atomic de Broglie wavelength is larger than the k itself,

$$\phi = \frac{1}{k^2}\frac{dk}{dr} > 1 .$$

When the potential is of the form $U_{\text{int}} = -C_n/r^n$, the ϕ takes a maximum $\phi_{\max}$ at a finite distance

$$r_{\max} = \left\{\frac{(n-2)mC_n}{(n+1)\hbar^2 k_0^2}\right\}^{1/n}.$$

Since the $\phi_{\max}$ goes to infinity as $k_0 \to 0$ for $n > 2$, the reflectivity is expected to approach unity when the normal incident velocity $v_n = \hbar k_0/m$ approaches zero [14,15]. The reflection of this type has been called quantum reflection and was observed on the reflection of He and H atoms on liquid helium surface [16,17] and also indirectly from the sticking coefficient of hydrogen on liquid He [18,19]. The quantum reflection is also expected on solid surfaces. Kasevich *et al.* [20] observed the deviation from the classical reflection of alkali atoms on the potential barrier created by the evanescent light above a glass surface. There have been theoretical discussions on the quantum mechanical effect in various configurations [21–23]. However, to our knowledge, an experiment that shows a high reflectivity on a solid surface has not been reported due to the extremely low velocity required to observe the phenomenon.

We overcame this difficulty by using a well-collimated atomic beam that was released from a very small trap of neutral atoms. The reflectivity of metastable Ne atoms on Si and BK7 glass surfaces was studied. The atomic beam hit the surface at a very shallow angle, and the v_n dependence of the reflectivity was measured by varying the incident angle. We used a microchannel plate (MCP) detector, which enabled us to distinguish unambiguously specularly reflected atoms from randomly scattered ones even at very low reflectivity. By using a beam with collimation better than 3×10^{-4} rad at the sample, we could measure the reflectivity at a velocity as small as 1 mm/s and observed reflectivity higher than 30%.

The experimental setup is shown in Fig. 1. Metastable neon atoms in the $1s_5[{}^3P_2]$ state were cooled and trapped in a magneto-optical trap. The diameter of the trapped atoms was typically 100 μm. A 598 nm laser beam was focused into the cloud of trapped atoms and pumped approximately half of the $1s_5$ atoms optically into the $1s_3$ state. The remaining half decayed to the ground state by emitting a vacuum ultraviolet (VUV) photon. The $1s_3$ atoms were freed from the trapping potential, fell along a parabolic path pulled by gravity and illuminated uniformly a mask that was placed 37 cm below the trap. The mask had five holes (see Fig. 2). Atoms that passed through the middle hole hit a silicon or a BK7 glass plate and were scattered or quenched. The hole was aligned exactly along the vertical line from the trap, and its diameter was

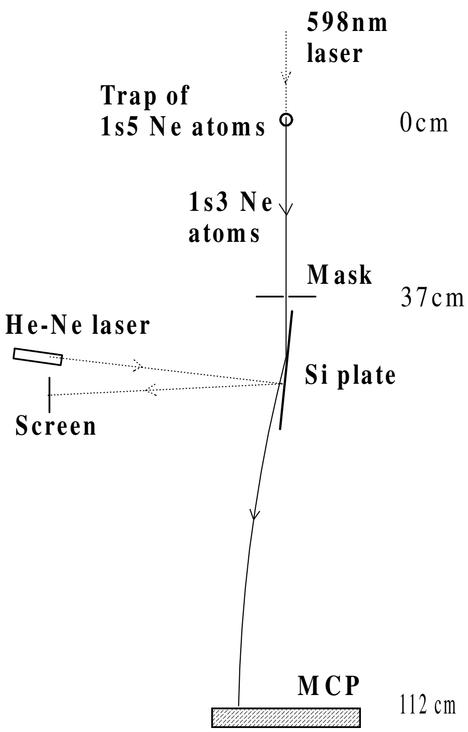

FIG. 1. The cross-sectional view of the experimental setup. The $1s_3$ metastable neon atoms were generated by focusing an optical pumping laser at 598 nm into the trap of the $1s_5$ atoms. The mask, the top of the reflecting plate and the MCP were placed 37, 39, and 112 cm below the trap, respectively.

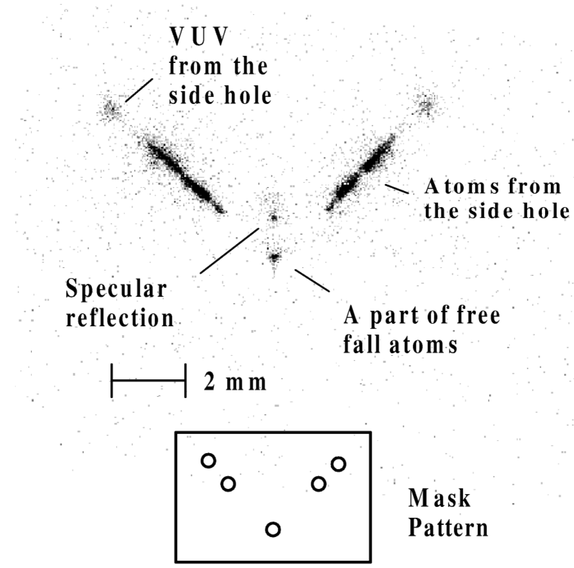

FIG. 2. The pattern of the mask and the image on the MCP. The hole in the center below was aligned exactly along the vertical line from the trap. Its diameter was 0.1 mm. The four other holes are at a distance of 1.4 and 2.0 mm from the central hole. Atoms that passed through those holes did not hit the surface, and their pattern on the MCP served to align the central hole, to determine the velocity distribution of the source and to calibrate the beam flux of the central hole. The VUV and atomic images do not overlap due to the difference in trajectory, except those from the central hole. The image of the free fall atoms were created by atoms that missed the plate. The vertical point is located slightly below this image. The image shows the case of $v_n = 3.8$ mm/s and without the 628 nm laser.

either 0.1 or 0.4 mm. The pattern of the scattered atoms was detected by the MCP that was placed 1120 mm below the trap. A clear spot arising from the specularly reflected atomic beam that had approximately the same beam divergence as the incident beam was observed in all velocity ranges. Atoms that passed other four holes hit the MCP directly. Since those holes were not on the vertical line, the atomic image on the MCP spread due to the velocity dispersion in the source. The image spread radially from the vertical line, and the velocity distribution was determined from its length, while the total intensity of the image was used to calibrate the relative intensity of the specularly reflected spot. The absolute reflectivity was obtained by dividing the relative intensity of the specularly reflected spot by that of the atoms from the middle hole when the plate was removed.

For a measurement at a larger angle, a 628 nm laser beam was superposed on the 598 nm optical pumping laser. The 628 nm laser produced a conical shape attractive potential for the $1s_3$ atoms around the trap, and cooled adiabatically the transverse velocity distribution. This increased the flux by an order of magnitude at the cost of a larger effective size of the beam source. Because of a large gravity acceleration, the velocity dispersion of atoms was reduced within 1% of the vertical velocity (approximately 3 m/s) at the height of the plate. The velocity dispersion due to the height difference along the plate was much larger and amounted to 20%.

A silicon or a BK7 glass plate was placed immediately below the pinhole. The silicon plate was of B-doped p-type with the resistivity of 10 Ω cm, and the surface had the (1,0,0) face. The length was 20 cm for the silicon and 17 cm for the BK7 plate. We also tried a silicon plate with the 7.8 mΩ cm conductivity and a plate without the oxidized surface layer. The result was nearly the same as that of the 10 Ω cm plate. We show only the result of the 10 Ω cm plate. The relative angle between the plate and the atomic beam was determined by reflecting a He-Ne laser beam onto the surface. The spatial distribution of the $1s_3$ atoms on the MCP was recorded on a video tape and simultaneously analyzed by using a personal computer. The vacuum was typically 2×10^{-7} Pa. The plate was not processed after installation into the vacuum chamber.

Figure 2 shows the image when operated without the 628 nm laser. The figure was taken with a continuous atomic beam and contained spots by the 74 nm VUV photons that were emitted from the source. The VUV images were either weak or well separated in space from the image of reflected atoms and caused no serious interference. However, in the real run the trapping laser, the optical pumping laser, and the discharge of the source were switched off every 64/60 s for 32/60 s. The data were accumulated during the switched-off period when no VUV photon hit the detector.

Figures 3 and 4 show the reflectivity as a function of v_n incident on the silicon surface and on the BK7 glass surface, respectively. Both figures are qualitatively similar. The reflectivity decreased monotonically with v_n. On the high velocity side between 10 mm/s and 30 mm/s, the reflectivity decreased nearly exponentially. Its decay constant was 5.5 s/mm for silicon and 7.5 s/mm for BK7. On the lower velocity side the reflectivity changed more rapidly and seemed to approach unity as $v_n \to 0$ with a finite slope. The latter behavior showed clearly that the reflection was not caused by a positive potential barrier. The accuracy of the measurement was approximately $\pm 20\%$ in the higher velocity region, which was estimated from the scattering of the experimental data and the statistical error. In the lower velocity region below 5 mm/s the error was larger due to the positioning error of the plate relative to the pinhole. At about $v_n = 1$ mm/s the error was nearly $\pm 50\%$. In the region $v_n < 2$ mm/s, the length of the plate did not cover the entire atomic beam, and the reflectivity was corrected according to the geometrical ratio.

For a perfect conductor the coefficient C_4 of the Casimir potential is [2]

$$C_4 = C_C \equiv \frac{3\hbar c \alpha}{32\pi^2 \epsilon_0}.$$

By using the polarizability of $\alpha = 2.8 \times 10^{-39}$ F m^2 [24], one get $r_{\max} = 1$ μm at the velocity of 1 mm/s. Since $\lambda/(2\pi)$ is of the order of 0.1 μm, this suggests that the reflection in the low velocity side is determined by the r^{-4} potential, while in the high velocity side it is governed by the potential in the transition region between the r^{-4} and r^{-3} dependence.

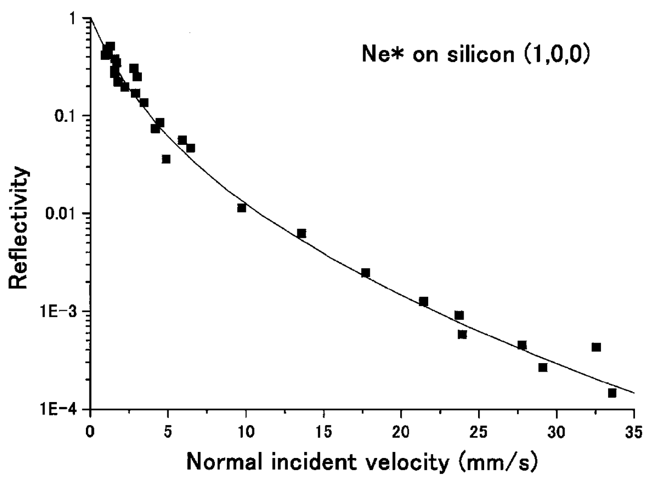

FIG. 3. The reflectivity vs the normal incident velocity on the Si(1,0,0) surface. The solid curve is the reflectivity calculated by using the potential Eq. (1) with $\lambda = 0.4$ μm and $C_4 = 6.8 \times 10^{-56}$ J m^4, which corresponds to $\alpha = 2.0 \times 10^{-39}$ F m^2 of Casimir's theory.

To obtain quantitative comparison we integrated numerically the wave equation with several model potentials. We calculated the reflectivity by assuming that, at a very short distance $r_s \sim$ nm, the wave function contained only the wave moving towards the surface, $\Psi = A \exp(-i \int k\, dr)$, where A is a slowly varying function of r compared to the phase variation. The reflectivity $R(v_n) = |B/A'|^2$ was obtained from the solution at a large distance $\Psi = A' \exp(-ik_0 r) + B \exp(ik_0 r)$. To test the influence of r_s on the reflectivity we calculated $R(v_n)$ by varying r_s from $0.3 r_{\max}$ to $10^{-2} r_{\max}$ for the r^{-3} and r^{-4} potentials. The reflectivity did not vary more than 3%. Since the WKB approximation improves at a smaller r, we assumed that the influence on the choice of r_s was small as long as $r_s \ll r_{\max}$. We used a fixed value in the calculation that corresponds to $r_s = 2.3$ nm when $C_4 = C_C$ was assumed. This value was more than an order of magnitude smaller than $r_{\max}$ and roughly equal to the roughness of the Si surface. We tried to fit the slopes of Figs. 3 and 4 in the low velocity range, $v_n < 8$ mm/s, with the r^{-4} potential. Using $C_4 = C_C$ for silicon we obtained $\alpha = (1.9 - 0.9 + 1.3) \times 10^{-39}$ F m^2, which is in agreement with the value $\alpha = 2.8 \times 10^{-39}$ F m^2 determined from the dc Stark effect by Noh *et al.* [24]. To derive α from the data of the BK7 glass we estimated the correction factor for dielectrics from the formula $C_4 = C_C \phi(\epsilon)(\epsilon - 1)/(\epsilon + 1)$ and the numerical plot of $\phi(\epsilon)$ by Dzyaloshinskii *et al.* and Spruch and Tikochinsky [25,26] as $C_4 \approx 0.51 C_C$. This value gave $(3.2 - 1.6 + 1.9) \times 10^{-39}$ F m^2.

A better fitting over the entire velocity range was obtained with the potential

$$U_{\text{int}} = -\frac{C_4}{(r + \lambda/2\pi) r^3}, \tag{1}$$

which satisfies approximately Casimir's theory [2] including the constant at two limiting distances $r \to 0$ and

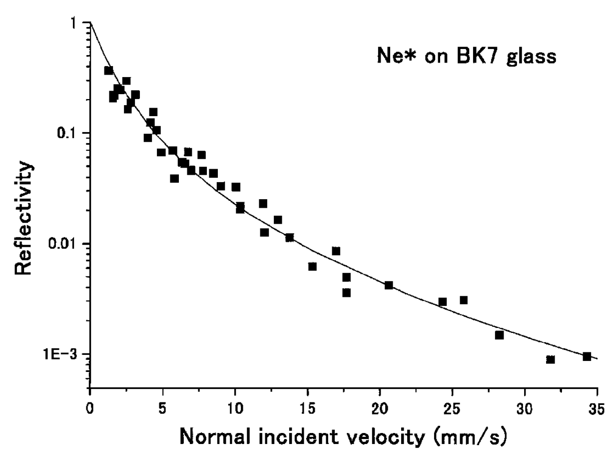

FIG. 4. The reflectivity vs the normal incident velocity on the BK7 glass surface. The solid curve is the reflectivity calculated by using the potential Eq. (1) with $C_4 = 7.3 \times 10^{-56}$ J m^4 and $\lambda = 5.0$ μm.

$r \to \infty$. The least squares fitting of the 43 data in Fig. 4 give $C_4 = 7.3 \times 10^{-56}$ J m^4 and $\lambda = 5.0$ μm. The range within σ confidence is $(4.2 - 22) \times 10^{-56}$ J m^4 for C_4 and 1.0–22 μm for λ. The $R(v_n)$ calculated with the values outside this range clearly showed systematic deviation from the experimental points. The same calculation for silicon give $C_4 = 6.7 \times 10^{-56}$ J m^4 and $\lambda \sim 0$. The range within σ confidence is $(6.7 - 8.4) \times 10^{-56}$ J m^4 for C_4 and 0–4.7 μm for λ. This C_4 give $\alpha = (2.0 - 2.5) \times 10^{-39}$ F m^2. Although the accuracy of the present experimental result is not sufficient for a detailed qualitative comparison, the above result shows that the specular reflection is caused by the quantum reflection from the van der Waals–Casimir potential.

The influence from the repulsive core potential was not observed. This is not unreasonable because the metastable $1s_3$ neon atom is quenched with high probability when it approaches within the reach of the core potential. Furthermore, the surface has a roughness of the order of several nm. Since the de Broglie wavelength of the atom that approaches near the surface is much smaller than the scale of the surface roughness, the atom senses the local variation and is scattered randomly. Since we detect only the specularly reflected component, the atom scattered on the core contributes little to the reflectivity. The effect of the core will become more prominent at a larger v_n, where the amplitude of the quantum reflection becomes closer to that of the core reflection. Our experimental accuracy was not sufficient to detect such an effect.

In conclusion we have shown clear evidence of specular reflection of atoms on a solid surface that was caused by the attractive Casimir potential. The reflectivity of larger than 30% was observed at the normal velocity of about 1 mm/s. The potential of the same form was found to fit the velocity dependence of the reflectivity on the BK7 glass surface. The present technique provides a method to study the interaction of a neutral particle with a solid surface in a wide range of distance from the surface and gives useful information for the designing of coherent surface atom-optics devices.

The author thanks J. Fujita of NEC for supplying silicon wafers. This work was partly supported by Grants in Aid for Scientific Research (11216202) from the Ministry of Education, Science, Sports and Culture.

[1] J. E. Lenard-Jones, Trans. Faraday Soc. **28**, 333 (1932).
[2] H. B. G. Casimir and D. Polder, Phys. Rev. **73**, 360 (1948).
[3] See, for example, G. Vidali *et al.,* Surf. Sci. Rep. **12**, 133 (1991).
[4] D. Raskin and P. Kusch, Phys. Rev. **179**, 712 (1969).
[5] A. Shih and V. A. Parsegian, Phys. Rev. A **12**, 835 (1975).
[6] A. Anderson *et al.,* Phys. Rev. A **37**, 3594 (1988).
[7] C. I. Sukenik *et al.,* Phys. Rev. Lett. **70**, 560 (1993).
[8] R. E. Grisenti *et al.,* Phys. Rev. Lett. **83**, 1755 (1999).
[9] H. Ito *et al.,* Phys. Rev. Lett. **76**, 4500 (1996); H. Ito *et al.,* in *Atom Optics*, edited by M. G. Prentiss and W. D. Phillips, SPIE Proceedings Vol. 2995 (SPIE, Bellingham, WA, 1997), p. 138.
[10] A. Landragin *et al.,* Phys. Rev. Lett. **77**, 1464 (1996).
[11] V. Sandoghdar *et al.,* Phys. Rev. Lett. **68**, 3432 (1992).
[12] M. Oria *et al.,* Europhys. Lett. **14**, 527 (1991).
[13] M. Chevrollier *et al.,* J. Phys. II (France) **2**, 631 (1992).
[14] C. Carraro and M. W. Cole, Prog. Surf. Sci. **57**, 61 (1998).
[15] R. B. Doak and A. V. G. Chizmeshya, Europhys. Lett. **51**, 381 (2000).
[16] V. U. Nayak, D. O. Edwards, and N. Masuhara, Phys. Rev. Lett. **50**, 990 (1983).
[17] J. J. Berkhout *et al.,* Phys. Rev. Lett. **63**, 1689 (1989).
[18] J. M. Doyle *et al.,* Phys. Rev. Lett. **67**, 603 (1991).
[19] I. A. Yu *et al.,* Phys. Rev. Lett. **71**, 1589 (1993).
[20] M. Kasevich *et al.,* in *Atomic Physics 12,* edited by Jens C. Zorn and Robert R. Lewis, AIP Conf. Proc. No. 233 (AIP, New York, 1991), p. 47.
[21] C. Henkel, C. I. Westbrook, and A. Aspect, J. Opt. Soc. Am. B **13**, 233 (1996).
[22] B. Segev, R. Cote, and M. G. Raizen, Phys. Rev. A **56**, R3350 (1997).
[23] E. G. Lima *et al.,* Phys. Rev. A **62**, 013410 (2000).
[24] H-R. Noh, K. Shimizu, and F. Shimizu, Phys. Rev. A **61**, 041601 (2000).
[25] I. E. Dzyaloshinskii, E. M. Lifshits, and L. P. Pitaevskii, Adv. Phys. **10**, 165 (1961).
[26] L. Spruch and Y. Tikochinsky, Phys. Rev. A **48**, 4213 (1993).